IMPROVEMENT OF THE ELECTROCHEMICAL BEHAVIOUR OF Zn-ELECTROPLATED STEEL USING REGENERATED Cr (III) PASSIVATION BATHS

J. García-Antón[1,*], R.M. Fernández-Domene[1], R. Sánchez-Tovar[1], C. Escrivà-Cerdán[1,3], R. Leiva-García[1,3], V. García[2], A. Urtiaga[2]

[1]IEC, Dpto. Ingeniería Química y Nuclear. Universitat Politècnica de València. C/ Camino de Vera s/n. 46022 Valencia, Spain. E-mail: jgarciaa@iqn.upv.es
[2]Departamento de Ingenierías Química y Biomolecular, Universidad de Cantabria, Av de los Castros, s/n., 39005, Santander, Cantabria, Spain
[3]School of Materials, University of Manchester, Manchester M13 9PL, UK

Abstract

Conversion coatings based on trivalent chromium are more sensitive to the presence of zinc and iron impurities than the chromate formulations. This fact contributes to a decrease in the quality of passivation and to the generation of a significant amount of hazardous liquid waste. Recently, a new eco-innovative process based on Emulsion Pertraction Technology (EPT) is being implemented at industrial scale for selectively removing Zn and Fe from spent passivation baths in order to enhance the lifetime of the Cr (III) baths. In this study, the effect of Zn and Fe removal on the electrochemical behaviour of Zn-electroplated steel samples was evaluated by means of polarisation curves and electrochemical impedance spectroscopy measurements at open circuit potential conditions in 3.5 g/L NaCl solutions. The main objective was to assess the benefits brought by EPT using electrochemical methods. Cr (III) passivation baths regenerated using the EPT process have been compared to the bath used in a local industry as well as to fresh and spent baths. According to the results, the samples passivated in the EPT regenerated bath showed a significant improvement in their electrochemical behaviour compared to the samples passivated in the spent baths. This study concluded the suitability of EPT for regenerating Cr(III) passivation baths.

Keywords: trivalent chromium; passivation baths; emulsion pertraction technology; Zn-electroplated steel.

1. Introduction

Chromate conversion coatings based on Cr (VI) chemicals have been widely used for many years to protect metals and alloys from corrosion [1, 2], in particular, to provide an extra protective film against corrosion and decorative finishing to electroplated zinc surfaces [3, 4]. The chemical passivation mechanism consists of the formation of a physical barrier between the metal/alloy substrate and the corrosive medium during immersion [5]. As a result of this, a passivation layer containing zinc oxides and hydroxides, zinc chromate and mixed Cr (III) and Cr (VI) oxides and hydroxides is formed.

However, the use of Cr (VI) compounds is considered carcinogenic for human health [6, 7] and causes serious environmental pollution; this is the reason why several research studies have focused on finding substitutes to Cr (VI) chemicals [1, 8-11].

Cr (III) passivation baths are used as an alternative to chromate conversion coatings. Although the substitutes reduce the toxicity of the used raw materials and of the produced wastes, they have several negative effects from the environmental and economic perspective [12]. The formulations based on Cr (III) need higher chromium concentrations and the presence of cobalt to provide equivalent properties to chromate-based passivation coatings. This fact implies a higher consumption of raw materials for the baths formulation. In addition, the Cr (III) baths are sensitive to the presence of Zn and Fe impurities, causing a decrease in the quality of passivation [13], formation of off-specification products and the generation of a significant amount of hazardous liquid waste when the passivation bath is replaced.

In order to enhance the lifetime of the baths and to improve the environmental and economical sustainability of Cr (III) passivation, a new eco-innovative process, is being developed based on Emulsion Pertraction Technology (EPT). EPT is able to separate Zn and Fe from the bath allowing Cr (III) and other relevant components such as cobalt to remain in the bath, i.e., preventing the loss of passivation properties. EPT combines liquid-liquid extraction with hollow fiber membrane contactors to extract and back-extract targeted compounds from an aqueous solution in one separation step. The fundamentals of EPT are explained in detail by Ho and Poddar [14] and Urtiaga et al. [15]. The main benefit of the process is that Cr (III) regeneration is conducted during passivation. This process for the regeneration of Cr (III) baths is being studied in detail at laboratory scale [16-19] and it has already been implemented at industrial scale [12]. Its environmental benefits were already assessed in a previous work [20]. However, the evaluation of the effectiveness of the EPT process from the corrosion protection perspective was lacked.

The main objective of this work is to evaluate the effectiveness of EPT on the electrochemical behaviour of Zn-electroplated steel samples by means of polarisation curves and EIS measurements. Cr (III) passivation baths regenerated using EPT are compared to freshly-made formulations, in-use baths and spent baths.

2. Experimental procedure

2.1. Material

Test specimens of 3.9 x 7.9 cm were cut from a Zn-electroplated steel sheet 0.1 cm thick. The sheet previously underwent the following surface treatments conducted at a local plating industry: chemical degreasing, rinsing in water, pickling, rinsing in water,

electrochemical degreasing, rinsing in water, Zn electroplating, rinsing with water, neutralising, passivation, rinsing in water and drying. Zn electroplating was conducted using 2.6 A dm^{-2} in alkaline media. The passivation step lasted 1 min at pH~1.8. Four passivating baths were tested for comparison: a fresh bath, the bath used at the company (in-use bath), spent bath and a bath regenerated using EPT. The fresh bath corresponded to a readily prepared formulation. The in use and spent baths were of the same chemical formulation as the fresh one and represented different degrees of usage. The bath regenerated using EPT resulted from the regeneration of the spent bath using the EPT process. The content of impurities was decreased until the Fe and Zn concentration levels were similar to the ones presented in the in use formulation. **Table 1** indicates the composition of the baths in terms of Zn (II), Fe (total) and Cr (III) concentrations.

2.2. Raman Spectroscopy

Prior to the electrochemical tests, the samples were examined by Raman spectroscopy ("*Witec 300R^{+} Raman microscope"*) in order to determine the presence of chromium oxides in the surface film. The samples were illuminated by a 632 nm neon laser with a magnification factor of 500x, the intensity of the laser being fixed. Several areas of the different samples were examined and the spectra were averaged.

2.3. Potentiodynamic polarisation curves

The potentiodynamic polarisation curves were determined using a potentiostat "AUTOLAB PGSTAT302N". The tests were carried out in a three-electrode cell. The potential of the working electrode was measured against a silver-silver chloride with 3M KCl reference electrode. The auxiliary electrode was a platinum electrode. The polarisation curves were obtained in a naturally aerated 3.5 g/l NaCl aqueous solution,

starting from a cathodic potential of – 1100 $mV_{Ag/AgCl}$ to 500 $mV_{Ag/AgCl}$ at 0.5 mV/s sweep rate.

During the electrochemical test, the surface area in contact with the NaCl solution was 0.626 cm^2.

2.4. Electrochemical Impedance Spectroscopy (EIS) Measurements

The EIS measurements were conducted at open circuit potential (OCP) in the 3.5 g/l NaCl solution after 1, 24, 48 and 144 hours of immersion in order to study the evolution of the film with time. The voltage perturbation amplitude was 10 mV in the frequency range of 100 kHz to 10 mHz. The temperature of the solution was 25 ºC.

3. Results and discussion

3.1. Raman spectra

Figure 1 shows the Raman spectra obtained by spotting a laser beam on the different samples. The peak of chromium oxide (540 cm^{-1}) [21] can be clearly observed in the specimen immersed in the fresh bath. In the other samples there is a decrease in the intensity of this peak with the following order: EPT-regenerated bath, in-use bath and spent bath. According to Rosalbino et al. [8], about 40% of the chromium in the Cr (III) conversion coatings is in the form of $Cr(OH)_3$, while about 60% is in the form of Cr_2O_3. Therefore, it is expected more concentration of Cr_2O_3 in the samples treated in baths with lower concentration of impurities (Zn, Fe). Therefore, the presence of chromium oxides decreases with the increase of the concentration of Zn and Fe impurities in the passivation bath (**Table 1**).

3.2. Potentiodynamic polarisation curves

The potentiodynamic polarisation curves of the passivated Zn electroplated steel samples immersed in the 3.5 g/L NaCl solution are shown in **Figure 2**. It is noteworthy that the surface treatments do not promote the existence of a passive region with constant values of anodic current density. Nevertheless, there are differences between the polarisation curves, the most important being the value of the anodic current densities. The specimen that was immersed in the fresh passivation bath had the lowest anodic current density value. Similarly, the anodic current densities of the samples treated in the regenerated and in-use baths are lower than when the spent formulation is used. These results indicate that the regeneration of the spent bath has a positive effect on the protective properties of the surface layer formed on the Zn electroplated sample.

3.3. EIS measurements

In order to better characterise the electrochemical behaviour of the Zn-electroplated specimens passivated with the baths under study, EIS measurements were performed at open circuit potential and at different immersion times in the 3.5 g/L NaCl solution.

Figures 3 to 6 show the evolution of the Bode-magnitude and Bode-phase (Figs a), and Nyquist (Figs b) plots with immersion time in the NaCl solution. The electrochemical impedance spectra reveal that the characteristics of the Cr(III) surface layer were similar, presenting a somewhat unfinished capacitive arc which is immersion time dependent. This feature is often considered as the response of an inhomogeneous film composed of a compact inner layer and a less compact (porous) outer layer [22-25]. However, other authors have proposed that the unfinished capacitive arc observed in coatings on electroplated steels is mainly due to the presence of a corrosion-resistant coating and a diffusion effect [26]. In this way, the modelling of the impedance data using an

equivalent circuit is necessary to explain the differences in the structure and corrosion resistance of the Zn electroplated steel passivated in the baths under study.

The Bode-phase plots show in general, two time constants, at high- and low-frequencies. All phase angles are lower than 90º; such behaviour can be interpreted as a deviation from ideal capacitor behaviour. Therefore, the use of a constant phase element (CPE) was necessary to account for the non-ideal behaviour of the capacitive elements [27]. Impedance of this element is then defined as [28]:

$$Z_{CPE} = \frac{1}{Q \cdot (j\omega)^{\alpha}} \quad (1)$$

where Q is the CPE constant, ω is the angular frequency (rad/s), j^2=-1 is the imaginary number and α is the CPE exponent. Depending on α, CPE can represent resistance (α=0, Z_0=R), capacitance (α=1, Z_0=C), or Warburg impedance (α=0.5, Z_0=W).

The equivalent electric circuit (EEC) represented in **Figure 7** was used to describe the impedance behaviour of a porous coating [3, 26, 29]. In the present work, this EEC has been used to model the results of the Zn electroplated steel samples passivated in the different baths. The results suggest that the surface film formed on the specimens consisted of a porous outer layer and a less defective inner layer inside the pores. The physical interpretation of this model may change depending on the used bath and on the immersion time, as well. In general, R_S is the resistance of the bulk solution, C_1 is the capacitance of the porous outer layer, R_1 is the solution resistance inside the pores of the outer layer, and C_2 and R_2 are respectively the capacitance and the resistance of the inner layer, including the possible existence of some defects. With increasing

immersion times, the inner layer becomes more defective leading to the appearance of pores so the electrolyte is able to reach the underlying metal. Therefore, C_2 and R_2 represent the active corrosion process taking place at the metal (Zn) substrate/electrolyte interface [30-32]. The diffusion element presented in the equivalent circuit in **Figure 7**, Z_W, represents a Warburg impedance inside the defects of the inner layer. The Warburg impedance used in the present study models dimensional diffusion of the electrolyte through a layer of finite thickness (the pores length) with absorbing boundary condition [26], whose equation is:

$$Z_W = \frac{R_W \tanh\left(B\sqrt{j\omega}\right)}{B\sqrt{j\omega}} \quad (2)$$

where $B = \delta/(D)^{1/2}$, D is the diffusion coefficient of the electrolyte through the pores, δ is the diffusion layer thickness and R_W is the Warburg resistance.

The schematic representation of the physical model, including the equivalent circuit, is shown in **Figure 8**. At short immersion times (**Figure 8a**), the inner layer is more compact and has small pores that cannot reach the metal surface. In this case, R_2 and C_2 are related to the protective properties of this layer. However, with increasing immersion times, pores in the inner layer become larger and the electrolyte can penetrated through this layer to the underlying metal surface (**Figure 8b**), so R_2 and C_2 represent a charge-transfer process of active corrosion at the metal (Zn) substrate/electrolyte interface. In all cases, a Warburg impedance appears as a consequence of the electrolyte diffusion inside the pores of the inner layer.

The interfacial capacitance (C_1) values were calculated using the expression given by Brug [27]:

$$Q_1 = C_1^{\alpha_1}\left(R_s^{-1} + R_1^{-1}\right)^{1-\alpha_1} \quad (3)$$

And the CPE_2 elements, Q_2, were converted into a pure capacitance, C_2 by means of the following expression:

$$C_2 = \frac{\left(Q_2 \cdot R_2\right)^{1/\alpha_2}}{R_2} \quad (4)$$

The electrical parameters were obtained by adjusting the experimental data shown in **Figures 3 to 6** and are summarised in **Table 2** as a function of the immersion time in the different passivation baths. In all cases, the resistance at very high frequencies, which corresponds to the uncompensated resistance of the solution, R_s, takes values between 133 and 189 Ω cm^2.

Table 2 indicates that the C_1 values of the Zn-electroplated samples passivated in the different baths are in general very low, of the order of μF cm^{-2} or even lower. This can be related to the presence of a thin Cr(III)-based surface film [5, 33, 34]. It can also be observed that, in general, the capacitance of the chromium layer (C_1) tends to increase with immersion time in the NaCl solution. This increase can be related to the water uptake of the coating, leading to an increase in the number of pores [30, 35]. The resistance of the solution in the porous of the outer layer, R_1, gradually decreases with the immersion time in the electrolyte (**Table 2**), indicating an increase in the number of heterogeneities in the coating [30, 35]. The values associated with the charge transfer

process taking place at the substrate/electrolyte interface, C_2, increase with the immersion time for all samples. Although for those samples passivated in the used and spent baths, the C_2 values are of the order of mF cm^{-2} (**Table 2**), which is mainly associated with the interfacial corrosion processes [30, 36]. Besides, C_2 increases significantly after 24 and 48 h of immersion in the electrolyte, which indicates an increase of the real interfacial area due to the formation of corrosion products on the substrate [36]. The decrease of C_2 at long immersion times (144 h), specially observed in the samples treated in the used and spent baths, may be related to the reduction of the interfacial area due to the partial dissolution of the corrosion products. R_2 values decrease with immersion time in all electrolytes, indicating less resistance to charge transfer, which means that the inner film's electrical conductivity increases as a result of the corrosion processes. In this sense, the corrosion reaction is assumed to take place at the bottom of pores, leading to a decrease in the resistance associated with the inner layer and an increase of C_2, as a result of enlargement of pores (**Figure 8b**). In addition, the values of the resistance inner layer R_2 are in all cases, significantly larger than the values associated with the outer porous layer (R_1), which is consistent with the chosen physical model (**Figure 7**). The parameter associated with the Warburg impedance, R_w decrease clearly with the immersion time (**Table 2**). This fact is an indication that the protective properties of the surface layer worsen, which is also related to the increase in the number of defects within the inner layer. Thus, the increase in the immersion time leads to deterioration of the zinc substrate as a consequence of the corrosion process taking place at the interface.

In order to compare the corrosion resistance of the samples passivated with the different baths, the total polarisation resistance, R_P, was obtained as the sum of the resistances R_1

and R_2, as well as R_w in the case of the specimens immersed in the in-use and spent baths. **Figure 9** shows the development of these values with immersion time in the 3.5 g/L solution. It can be observed that R_P decreases as immersion time increases, indicating worse protective properties of the Cr(III) layer as a consequence of corrosion attack to the protective coating. The highest R_P value corresponds to the sample passivated with the fresh bath, followed by the specimens immersed in the in-use and regenerated baths; the latter presents higher R_P values than the former, this indicates that the conduction of the regeneration step tends to improve the corrosion protection of the Zn-electroplated steel. Finally, the Zn-electroplated steel passivated with the spent bath presents the worst R_P value, indicating the poorest corrosion resistance.

The main differences among the passivation baths are related to their content in Zn and Fe, as shown in **Table 1**. Therefore, the presence of these impurities has a strong influence on the electrochemical properties of the samples treated in the different baths. This fact demonstrates the importance of designing a system capable of continuously removing these impurities in order to lengthen the lifetime of the bath and also to avoid the generation of off-specification products.

In order to understand how the presence of Zn in the passivation bath can affect the formation of the chromium-conversion coating it is important to better understand the mechanism of chromium deposition. When a Zn specimen is immersed in Cr (III) formulations, the metal undergoes redox reactions induced by the presence of microanodic and microcathodic zones on its surface. The formation of the conversion layer goes through the following different stages [8, 37]:

a) Zinc oxidation:

$$Zn \rightarrow Zn^{2+} + 2\ e^{-} \quad (5)$$

b) Hydrogen reduction:

$$2H^{+} + 2\ e^{-} \rightarrow H_2 \quad (5)$$

c) Local pH increase, which leads to the precipitation of chromium and Zn hydroxides.

Hence, the presence of Zn impurities affects the passivation process in two ways: decreasing the rate of Zn redox dissolution and increasing the presence of zinc hydroxides instead of chromium hydroxides in the conversion coating. Fe impurities can also interfere in the process of formation and precipitation of chromium hydroxides. These processes lead to a decrease in the corrosion resistance of the samples, as shown in **Figure 9**. Therefore, low concentrations of Zn and Fe in the passivation bath improve the properties of the conversion coating.

The presence of impurities also affects the environmental performance of the passivation process. The higher the amount of impurities the higher the amount of chromium required to obtain the same corrosion protective property. Consequently more original formulation is consumed to obtain the passivation bath and more natural resources in terms of materials, energy and water are used to produce the Cr (III) formulation. Other negative aspects caused by the presence of impurities in the bath are well explained in a the previous work. [20].

To evaluate the convenience of coupling an EPT step to the passivation bath in order to improve the protective properties of the electroplated steel, the ratios ($Rp_{EPT}/Rp_{SpentBath}$) and ($Rp_{InUse}//Rp_{SpentBath}$) have been calculated in **Table 3**. A reduction of 55% in the

amount of Zn used in the passivation bath (**Table 1**) increases R_p by a factor of 4.12 (0 hours), 2.90 (24 hours), 3.46 (48 hours) and 3.00 (144 hours). The highest enhancement is observed at short immersion times in the NaCl solution. These ratios are higher in the sample treated with the regenerated bath than in the sample treated with the in-use bath. Hence, according to the ratios shown in **Table 3**, EPT coupling to the passivation step significantly improved the protective properties of the passivated Zn electroplated steel compared to the spent bath. EPT regeneration is an eco-friendly, suitable treatment since it increases corrosion resistance as compared to the in-use passivation bath.

4. Conclusions

Emulsion Pertraction Technology (EPT) is an eco-innovative process able to separate Zn and Fe from Cr (III) passivation baths while retaining chromium and other relevant components. This work demonstrate by means of an electrochemical study, the importance of coupling an EPT step to the passivation bath to reduce the Zn and Fe impurities and consequently to improve the protective properties of the layers formed on electroplated steels.

Potentiodynamic polarisation results have shown that the regeneration of the spent bath has a positive effect on the protective properties of the surface layer formed on the Zn electroplated sample, since the values of the anodic current density are lower in the samples treated in the regenerated bath than in the spent bath. Further, the specimen immersed in the regenerated bath presented higher values of polarisation resistance (RP) than the specimens passivated with the in-use and spent baths.

This study also shows that the presence of chromium oxides on the samples surface decreases with the increase of zinc and iron concentrations in the passivation bath and that the presence of Fe and especially Zn impurities have a strong influence on the

electrochemical properties of the samples treated in the different baths, leading to a decrease in their corrosion resistance.

Finally, the results have revealed the importance of monitoring Zn impurities in the passivation baths. The concentration of Zn (II) in regenerated passivation baths should be reduced in the future to achieve conditions equivalent to those found in fresh passivation baths.

Acknowledgements

The authors would like to express their gratitude to the Project TIGI (FP7, European Commission, Grant agreement 218390) and to Dr. Asuncion Jaime for her translation assistance.

References

[1] X. Zhang, C. van den Bos, W. G. Sloof, A. Hovestad, H. Terryn, J. H. W. de Wit, Comparison of the morphology and corrosion performance of Cr(VI)- and Cr(III)-based conversion coatings on zinc, Surf. Coat. Technol. 199 (2005) 92-104.

[2] Z. Mekhalif, L. Forget, J. Delhalle, Investigation of the protective action of chromate coatings on hot-dip galvanized steel: role of wetting agents, Corros. Sci. 47 (2005) 547-566.

[3] K. Cho, V. Shankar Rao, H. Kwon, Microstructure and electrochemical characterization of trivalent chromium based conversion coating on zinc, Electrochim. Acta 52 (2007) 4449-4456.

[4] P. Campestrini, E. P. M. van Westing, J. H. W. de Wit, Influence of surface preparation on performance of chromate conversion coatings on Alclad 2024 aluminium alloy: Part I: Nucleation and growth, Electrochim. Acta 46 (2001) 2553-2571.

[5] T. Bellezze, G. Roventi, R. Fratesi, Electrochemical study on the corrosion resistance of Cr III-based conversion layers on zinc coatings, Surf. Coat. Technol. 155 (2002) 221-230

[6] C. R. Tomachuk, C. I. Elsner, A. R. Di Sarli, O. B. Ferraz, Morphology and corrosion resistance of Cr(III)-based conversion treatments for electrogalvanized steel, J. Coat. Technol. Res. 7 (2010) 493-502.

[7] C. S. Jeffcoate, H. S. Isaacs, A. J. Aldykiewicz, M. P. Ryan, Chromate in Conversion Coatings: A XANES Study of Its Concentration and Mobility, J. Electrochem. Soc. 147 (2000) 540-547.

[8] F. Rosalbino, G. Scavino, G. Mortarino, E. Angelini, G. Lunazzi, EIS study on the corrosion performance of a Cr(III)-based conversion coating on zinc galvanized steel for the automotive industry, J. Solid State Electrochem. 15 (2011) 703-709.

[9] X. Zhang, C. van den Bos, W. G. Sloof, H. Terryn, A. Hovestad, J. H. W. de Wit, Investigation of Cr(III) Based Conversion Coatings On Electrogalvanised Steel, Surf. Eng. 20 (2004) 244-250.

[10] F. Deflorian, S. Rossi, L. Fedrizzi, P. L. Bonora, EIS study of organic coating on zinc surface pretreated with environmentally friendly products, Prog. Org. Coat. 52 (2005) 271-279.

[11] G. Saravanan, S. Mohan, Corrosion behavior of Cr electrodeposited from Cr(VI) and Cr(III)-baths using direct (DCD) and pulse electrodeposition (PED) techniques, Corros. Sci. 51 (2009) 197-202.

[12] V. Garcia, W. Steeghs, M. Bouten, I. Ortiz, A. Urtiaga, Implementation of an eco-innovative separation process for a cleaner chromium passivation in the galvanic industry, J. Clean Prod. 59 (2013) 274-283.

[13] N. Zaki, Trivalent chrome conversion coating for zinc and zinc alloys, Met. Finish 105 (2007) 425-435.

[14] W. S. W. Ho, T. K. Poddar, New membrane technology for removal and recovery of chromium from wastewaters, Environ. Prog. 20 (2001) 44-52.

[15] A. Urtiaga, M. J. Abellán, J. A. Irabien, I. Ortiz, Membrane contactors for the recovery of metallic compounds: Modelling of copper recovery from WPO processes, J. Membr. Sci. 257 (2005) 161-170.

[16] N. Diban, R. Mediavilla, A. Urtiaga, I. Ortiz, Zinc recovery and waste sludge minimization from chromium passivation baths, J. Hazard. Mater. 192 (2011) 801-807.

[17] A. Urtiaga, E. Bringas, R. Mediavilla, I. Ortiz, The role of liquid membranes in the selective separation and recovery of zinc for the regeneration of Cr(III) passivation baths, J. Membr. Sci. 356 (2010) 88-95.

[18] N. Diban, V. García, F. Alguacil, I. Ortiz, A. Urtiaga, Temperature Enhancement of Zinc and Iron Separation from Chromium(III) Passivation Baths by Emulsion Pertraction Technology, Ind. Eng. Chem. Res. 51 (2012) 9867-9874.

[19] V. Garcia, N. Diban, E. Bringas, R. Ibañez, I. Ortiz, A. M. Urtiaga, The Use of Emulsion Pertraction Technology as an Eco-innovative Membrane Process for the Galvanic Industry, Procedia Eng. 44 (2012) 187-190.

[20] V. Garcia, M. Margallo, R. Aldaco, A. Urtiaga, A. Irabien, Environmental Sustainability Assessment of an Innovative Cr (III) Passivation Process, ACS Sustain. Chem. Eng. 1 (2013) 481-487.

[21] D. Thierry, In-situ Raman spectroscopy combined with X-ray photoelectron spectroscopy and nuclear microanalyisis for studies of anodic corrosion film formation on Fe-Cr single crystals, J. Electrochem. Soc. 135 (1988) 305-310.

[22] S. L. De Assis, S. Wolynec, I. Costa, Corrosion characterization of titanium alloys by electrochemical techniques, Electrochim. Acta 51 (2006) 1815-1819.

[23] J. Pan, C. Leygraf, R. F. A. Jargelius-Pettersson, J. Linden, Characterization of high-temperature oxide films on stainless steels by electrochemical-impedance spectroscopy, Oxid. Met. 50 (1998) 431-455.

[24] K. Jüttner, Electrochemical impedance spectroscopy (EIS) of corrosion processes on inhomogeneous surfaces, Electrochim. Acta 35 (1990) 1501-1508.

[25] S. Yagi, A. Sengoku, K. Kubota, E. Matsubara, Surface modification of ACM522 magnesium alloy by plasma electrolytic oxidation in phosphate electrolyte, Corros. Sci. 57 (2012) 74-80.

[26] N. T. Wen, C. S. Lin, C. Y. Bai, M. D. Ger, Structures and characteristics of Cr(III)-based conversion coatings on electrogalvanized steels, Surf. Coat. Technol. 203 (2008) 317-323.

[27] G. J. Brug, A. L. G. van den Eeden, M. Sluyters-Rehbach, J. H. Sluyters, The analysis of electrode impedances complicated by the presence of a constant phase element, J. Electroanal. Chem. Interfacial Electrochem. 176 (1984) 275-295.

[28] B. Evgenij, J. R. Macdonald, Impedance Spectroscopy: Theory, Experiment and Application, West Sussex, UK, 2005.

[29] J. Pang, A. Briceno, S. Chander, A Study of Pyrite/Solution Interface by Impedance Spectroscopy, J. Electrochem. Soc. 137 (1990) 3447-3455.

[30] C. Corfias, N. Pebere, C. Lacabanne, Characterization of a thin protective coating on galvanized steel by electrochemical impedance spectroscopy and a thermostimulated current method, Corros. Sci. 41 (1999) 1539-1555.

[31] C. R. Tomachuk, C. I. Elsner, A. R. Di Sarli, O. B. Ferraz, Corrosion resistance of Cr(III) conversion treatments applied on electrogalvanised steel and subjected to chloride containing media, Mater. Chem. Phys. 119 (2010) 19-29.

[32] V. Barranco, J. Feliu, S. Feliu, EIS study of the corrosion behaviour of zinc-based coatings on steel in quiescent 3% NaCl solution. Part 2: coatings covered with an inhibitor-containing lacquer, Corros. Sci. 46 (2004) 2221-2240.

[33] A. C. Bastos, M. G. S. Ferreira, A. M. Simões, Comparative electrochemical studies of zinc chromate and zinc phosphate as corrosion inhibitors for zinc, Prog. Org. Coat. 52 (2005) 339-350.

[34] J. Hazan, C. Coddet, Corrosion du zinc dans un mileu alcalin: effect d'un traitament de passivation chromique, J. Appl. Electrochem. 26 (1996) 203-209.

[35] X. Liu, J. Xiong, Y. Lv, Y. Zuo, Study on corrosion electrochemical behavior of several different coating systems by EIS, Prog. Org. Coat. 64 (2009) 497-503

[36] R. Touir, N. Dkhireche, M. Ebn Touhami, M. Lakhrissi, B. Lakhrissi, M. Sfaira, Corrosion and scale processes and their inhibition in simulated cooling water systems by monosaccharides derivatives: Part I: EIS study, Desalination 249 (2009) 922-928.

[37] M. P. Gigandet, J. Faucheu, M. Tachez, Formation of black chromate conversion coatings on pure and zinc alloy electrolytic deposits: role of the main constituents, Surf. Coat. Technol. 89 (1997) 285-291.

Tables captions

Table 1. Concentration of Cr (III), Zn (II) and Fe (total) in the baths used to passivate the Zn electroplated specimens.

Table 2. Electrical parameters obtained by fitting the experimental results of EIS to the circuit shown in **Figure 7**, for the samples passivated with the different baths and immersed in a 3.5 g/l NaCl at different times and at 25 ºC.

Table 3. Ratios for the regeneration treatments as function of immersion time in the 3.5 g/l NaCl solution. $Ratio_{EPT} = ([Rp_{EPT}/Rp_{SpentBath}]\cdot 100)$ and $Ratio_{InUse} = ([Rp_{InUse}/Rp_{SpentBath}]\cdot 100)$.

Figures captions

Figure 1. Raman spectra obtained for the samples treated in the following baths: fresh bath, EPT regenerated bath, in-use bath and spent bath.

Figure 2. Potentiodynamic polarisation curves of the specimens passivated in the baths under study and immersed in solutions of 3.5 g/L of NaCl.

Figure 3. Bode-magnitude and Bode-phase (a) and Nyquist (b) plots for the Zn electroplated steel samples passivated with the fresh bath and immersed in the solution of 3.5 g/L of NaCl at different times.

Figure 4. Bode-magnitude and Bode-phase (a) and Nyquist (b) plots for the Zn electroplated samples passivated with the EPT regenerated bath and immersed in the solution of 3.5 g/L of NaCl at different times.

Figure 5. Bode-magnitude and Bode-phase (a) and Nyquist (b) plots for the Zn electroplated steel passivated with the in-use bath and immersed in the 3.5 g/L of NaCl at different times.

Figure 6. Bode-magnitude and Bode-phase (a) and Nyquist (b) plots for the Zn electroplated steel samples passivated with the spent bath and immersed in the solution of 3.5 g/L of NaCl at different times.

Figure 7. Equivalent circuit proposed for all the passivation baths used in this work.

Figure 8. Schematic representation of the physical model, including the equivalent circuit, used to explained the EIS results obtained for the Zn electroplated steel samples at (a) short immersion times and (b) long immersion times.

Figure 9. Polarisation resistance values of the samples passivated in the different baths and their development with the immersion time in the 3.5 g/l NaCl solution.

Figure 1

Click here to download Figure: Figure 1.pdf

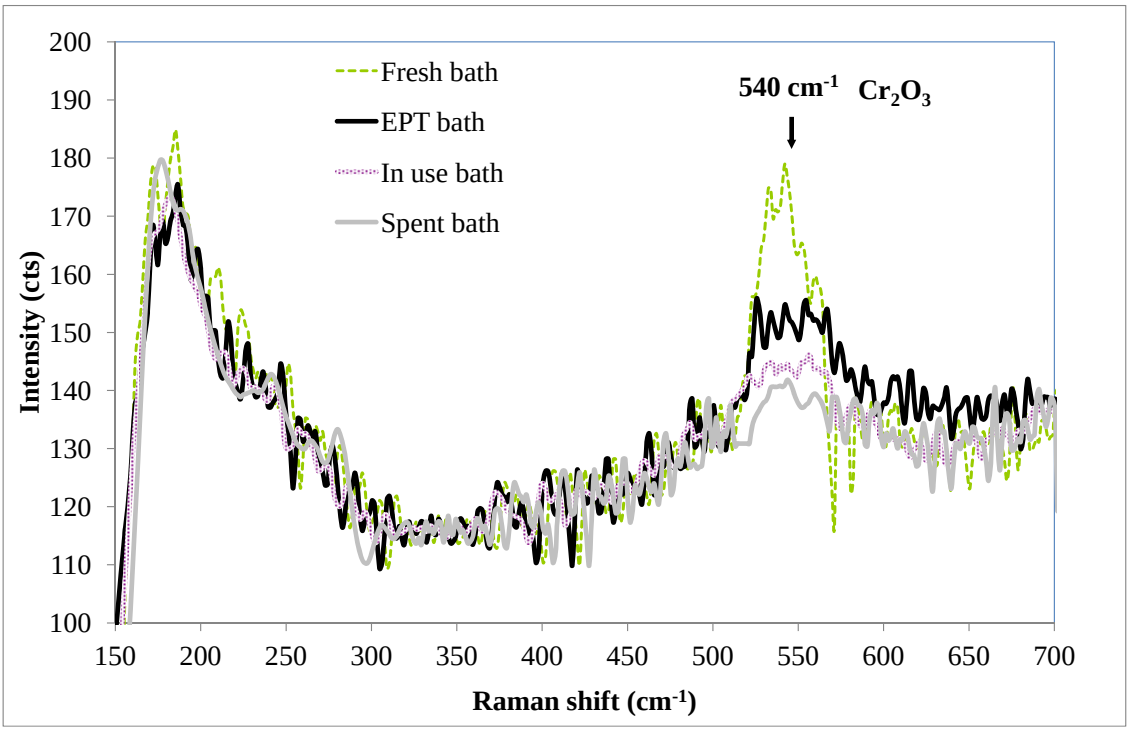

Figure 2

Click here to download Figure: Figure 2.pdf

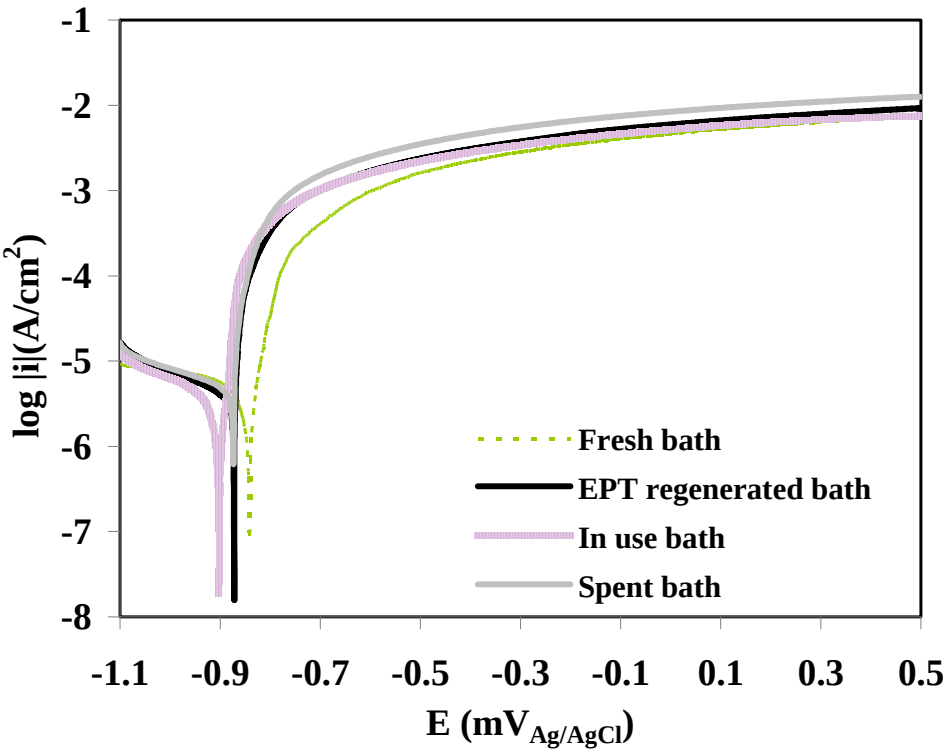

Figure 3

Click here to download Figure: Figure 3.pdf

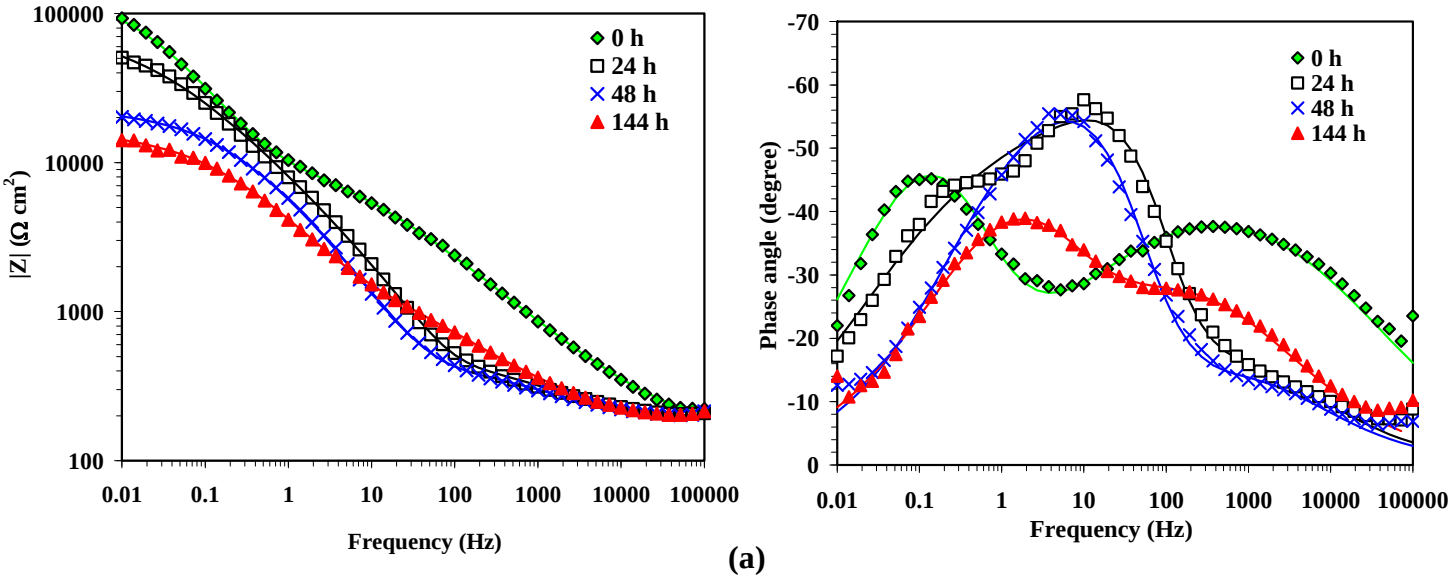

(a)

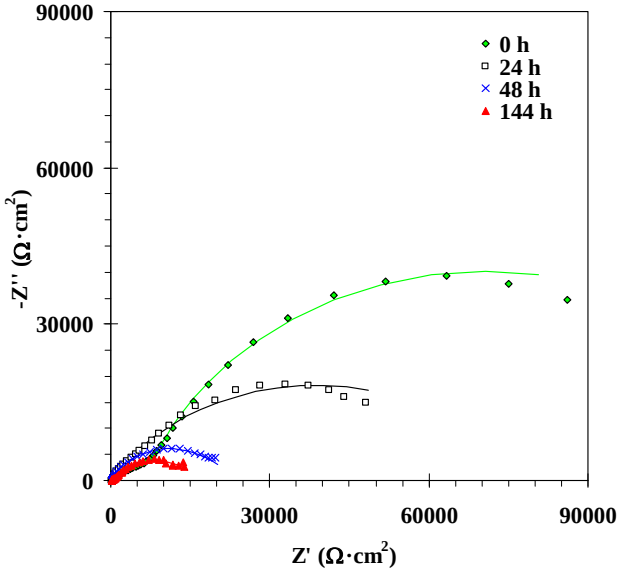

(b)

Figure 4

Click here to download Figure: Figure 4.pdf

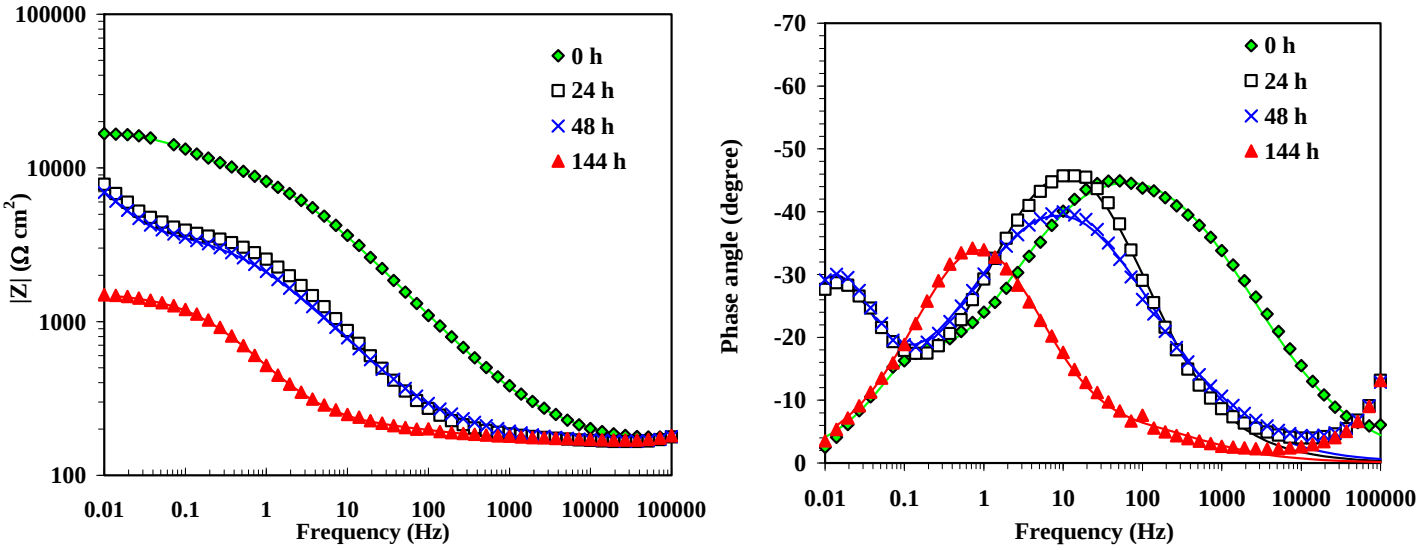

(a)

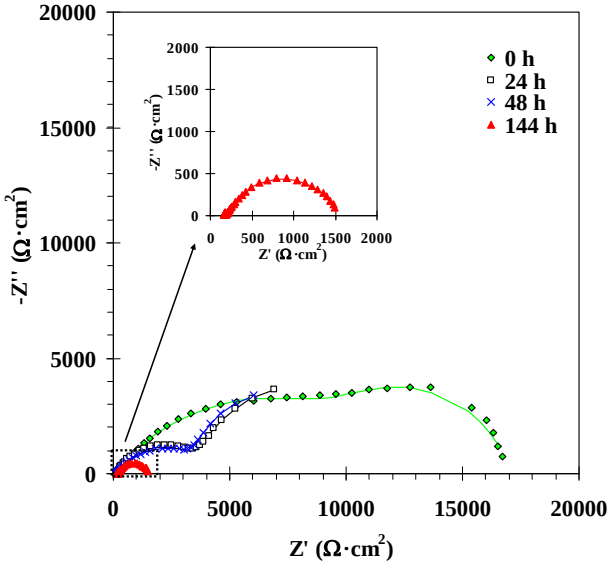

(b)

Figure 5

Click here to download Figure: Figure 5.pdf

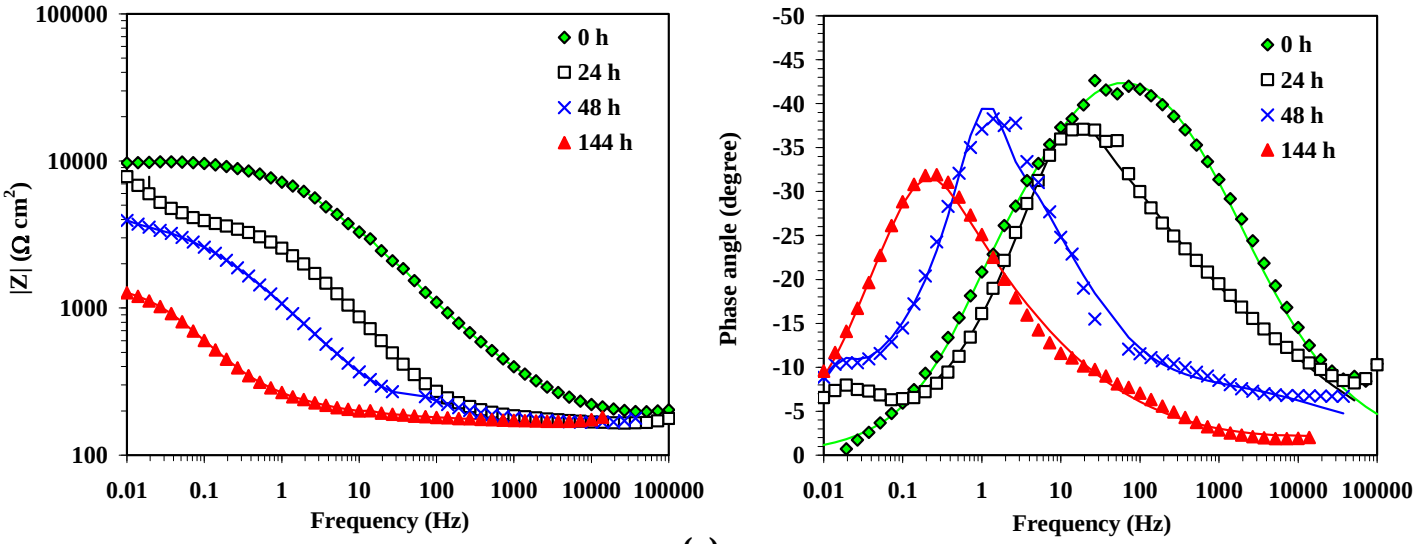

(a)

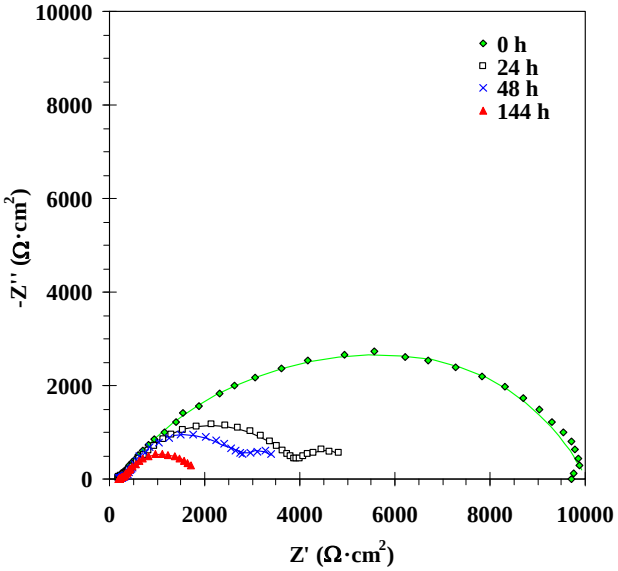

(b)

Figure 6

Click here to download Figure: Figure 6.pdf

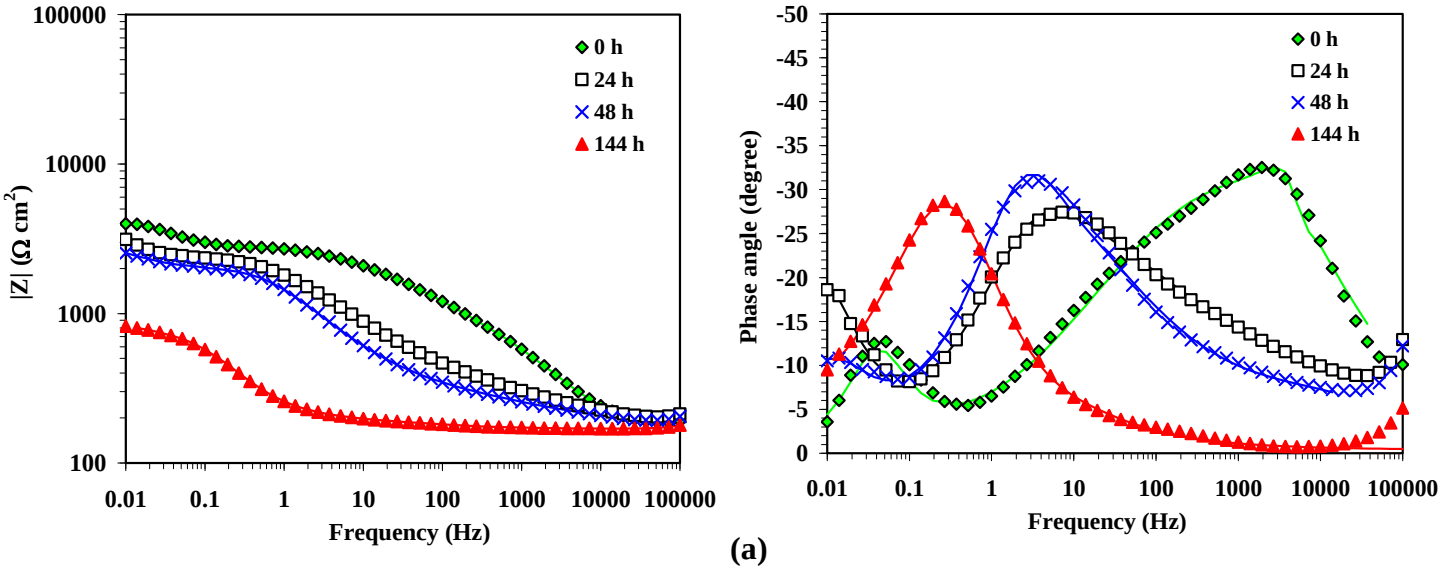

(a)

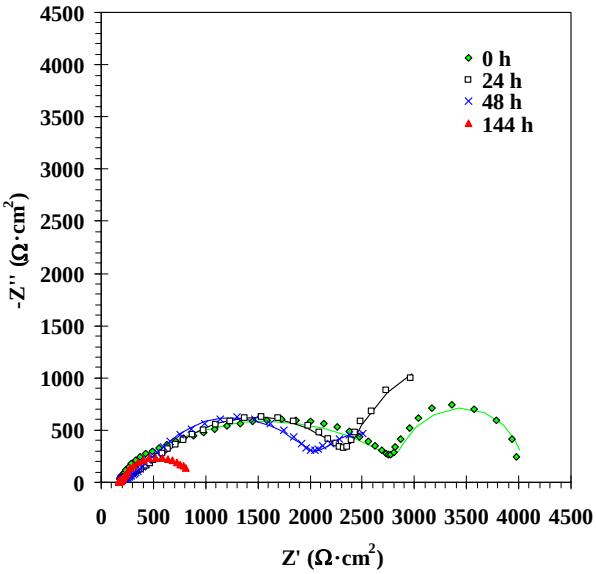

(b)

Figure 7

Click here to download Figure: Figure 7.pdf

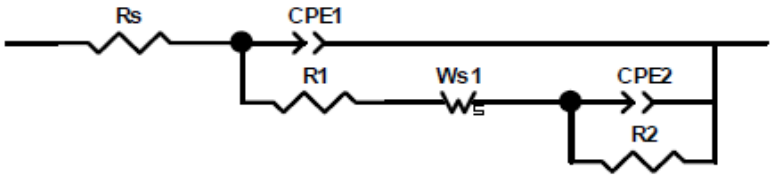

Figure 8
Click here to download Figure: Figure 8.pdf

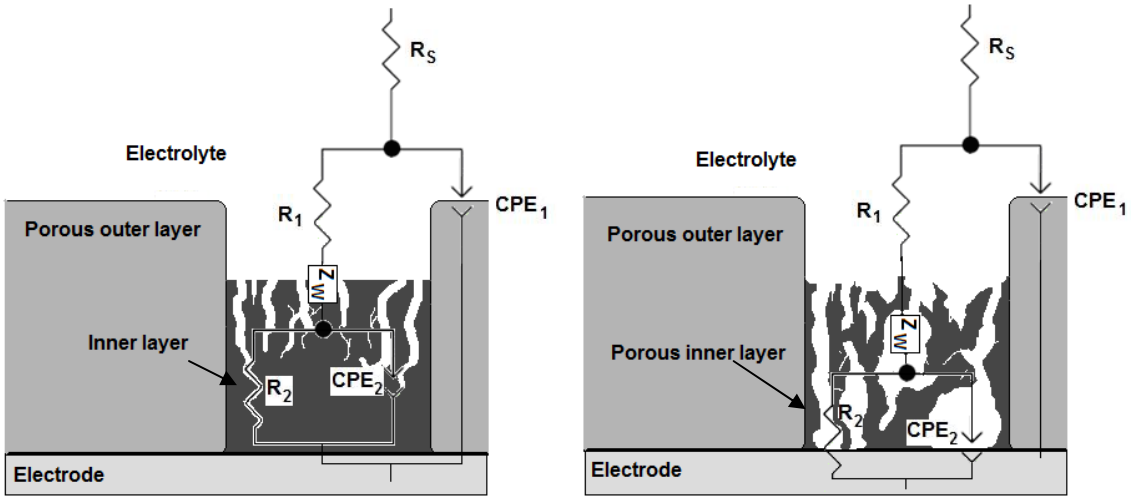

(a) **(b)**

Figure 9

Click here to download Figure: Figure 9.pdf

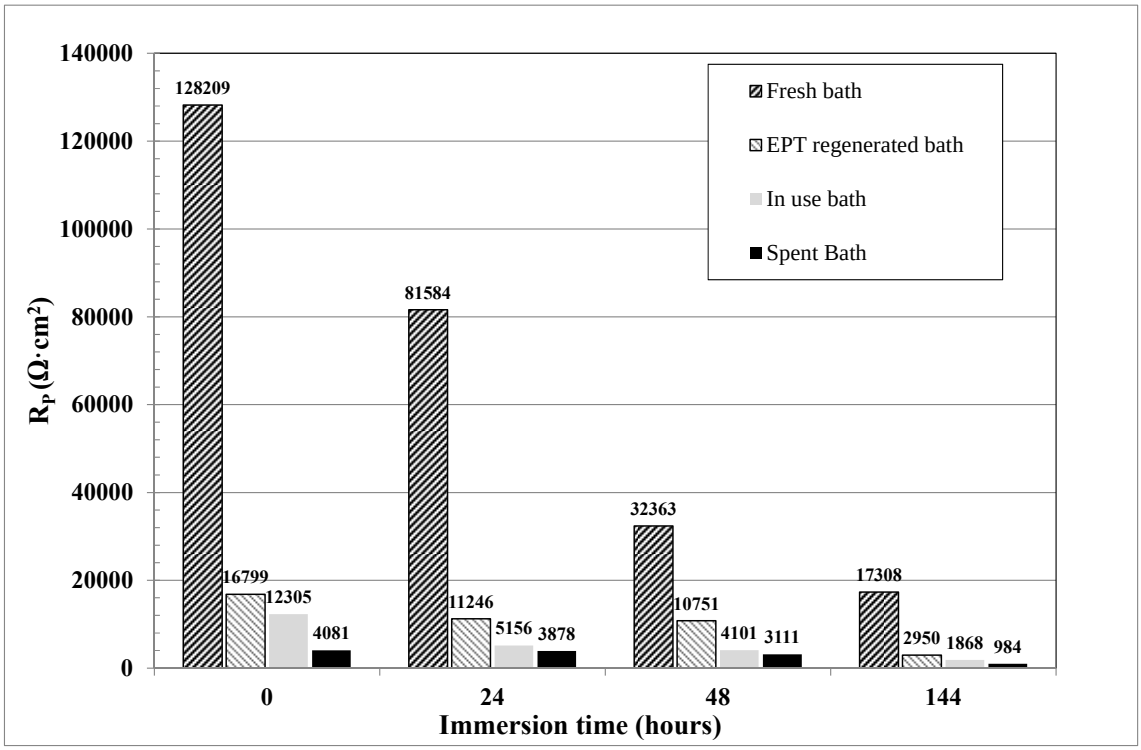

Table 1

Click here to download Table: Table 1.doc

	Cr (III) (mg/L)	Zn (II) (mg/L)	Fe (total) (mg/L)
Fresh bath	6729	< 0.3	0.72
EPT regenerated bath	6363	5824	11
In use bath	5400	7410	10
Spent bath	6402	13088	63.4

Table 2

Click here to download Table: Table 2.doc

Time	R_S/Ω cm^2	C_1/μF cm^{-2}	α_1	R_1/Ω cm^2	R_W/Ω cm^2	C_2/μF cm^{-2}	α_2	R_2/Ω cm^2	χ^2 (x10^{-3})
Fresh bath									
0h	138 ± 10	0.04 ± 0.01	0.52 ± 0.02	9649 ± 12	51381 ± 12	64 ± 2	0.92 ± 0.02	67041 ± 12	1.3
24h	189 ± 12	0.74 ± 0.03	0.55 ± 0.03	3046 ± 14	14360 ± 19	1 ± 0.1	0.92 ± 0.05	63989 ± 17	2.2
48h	186 ± 8	0.80 ± 0.05	0.57 ± 0.02	2798 ± 11	9226 ± 21	9 ± 0.9	0.91 ± 0.03	20153 ± 8	1.4
144h	165 ± 8	0.41 ± 0.02	0.48 ± 0.03	2074 ± 13	10144 ± 16	24 ± 3	0.95 ± 0.03	4925 ± 7	2.1
EPT regenerated bath									
0h	165 ± 7	0.33 ± 0.04	0.72 ± 0.01	572 ± 11	6616 ± 12	3 ± 0.5	0.58 ± 0.02	9446 ± 14	0.4
24h	166 ± 11	8.05 ± 0.3	0.74 ± 0.02	476 ± 15	8055 ± 16	3 ± 0.4	0.92 ± 0.03	2549 ± 9	7.9
48h	163 ± 9	4.20 ± 0.2	0.84 ± 0.01	218 ± 11	8254 ± 19	36 ± 4	0.74 ± 0.04	2116 ± 20	6.2
144h	170 ± 6	65.42 ± 3	0.67 ± 0.03	61 ± 9	1959 ± 18	865 ± 11	0.76 ± 0.03	760 ± 8	14.6
In use bath									
0h	176 ± 12	0.28 ± 0.02	0.59 ± 0.02	324 ± 12	4659 ± 21	0.10 ± 0.02	0.74 ± 0.02	7146 ± 19	2.2
24h	172 ± 8	0.26 ± 0.04	0.53 ± 0.03	284 ± 10	3866 ± 18	11679 ± 32	1.11 ± 0.15	834 ± 12	0.4
48h	175 ± 9	0.45 ± 0.01	0.40 ± 0.02	209 ± 4	3458 ± 23	87245 ± 25	1.027 ± 0.08	259 ± 10	1.8
144h	178 ± 10	0.07 ± 0.02	0.53 ± 0.01	28 ± 2	1419 ± 12	4570 ± 12	1.010 ± 0.05	243 ± 12	0.9
Spent bath									
0h	168 ± 10	0.11 ± 0.00	0.75 ±0.02	486 ± 11	2244 ± 19	400 ± 12	1.00 ± 0.02	1183 ± 17	0.9
24h	144 ± 8	0.03 ± 0.00	0.49 ±0.01	196 ± 8	2250 ± 13	1200 ± 21	1.00 ± 0.01	1288 ± 15	0.2
48h	152 ± 9	0.09 ± 0.00	0.44 ±0.02	124 ± 6	1963 ± 17	1960 ± 24	0.97 ± 0.02	872 ± 14	0.3
144h	166 ± 6	42.11 ± 2.00	0.50 ±0.03	30 ± 3	401 ± 13	190 ± 13	1.00 ± 0.01	387 ± 11	0.2

Table 3

Click here to download Table: Table 3.doc

Time (h)	$Ratio_{EPT}$ (%)	$Ratio_{InUse}$ (%)
0	412	302
24	290	133
48	346	132
144	300	193